Neuron, Vol. 11, 923–938, November, 1993, Copyright © 1993 by Cell Press

Transient Period of Correlated Bursting Activity during Development of the Mammalian Retina

R. O. L. Wong,* M. Meister,† and C. J. Shatz‡
Department of Neurobiology
Stanford University School of Medicine
Stanford, California 94305

Summary

The refinement of early connections in the visual pathway requires electrical activity in the retina before the onset of vision. Using a multielectrode array, we have shown that the spontaneous activity of cells in the neonatal ferret retina is correlated by patterns of periodically generated traveling waves. Here, we examine developmental changes in the characteristics of the waves and show that retinal ganglion cells participate in these patterns of activity, which are seen during the same period as synaptic modification in the lateral geniculate nucleus; that the waves subside gradually as the connectivity in the lateral geniculate nucleus stabilizes; and that their spatial structure allows for refinement of the retinotopic map, as well as for eye-specific segregation in the lateral geniculate nucleus.

Introduction

The formation of precise connections in the mammalian nervous system often relies on activity-mediated synaptic competition between axonal terminals for common postsynaptic sites (for recent reviews see Shatz, 1990; Constantine-Paton et al., 1990; Cline, 1991). In the visual system of the cat, the axons of prenatal retinal ganglion cells from both eyes grow to their primary target, the lateral geniculate nucleus (LGN), and initially arborize in a diffuse manner. Subsequently, the axonal arborizations from ganglion cells of each eye remodel and become restricted to give rise to eye-specific layers in this nucleus just before birth (Sretavan and Shatz, 1986).

Action potential activity from the retina is thought to be necessary for the eye-specific rearrangement of retinal input to the LGN because continuous blockade of such activity, by infusion of tetrodotoxin within the thalamus in the fetal cat, prevents the segregation of ganglion cell axons into layers (Shatz and Stryker, 1988; Sretavan et al., 1988). Since segregation occurs before birth in the cat, the activity from retinal ganglion cells that could drive this process must be occurring spontaneously; in the fetal cat, the retina has yet to develop photoreceptors, and no vision is possible (Greiner and Weidman, 1980). Evidence for such spontaneous action potential activity was recently provided by in vivo recordings from ganglion cells of the fetal rat (Galli and Maffei, 1988; Maffei and Galli-Resta, 1990) and in vitro recordings from early postnatal ferret retinas, at developmental stages equivalent to those of the fetal cat (Meister et al., 1991).

Neural activity appears to be necessary, but not by itself sufficient, for eye-specific segregation. Rather, the timing and pattern of firing are critical. For instance, in order for LGN axon terminals to segregate into ocular dominance columns in the visual cortex, action potentials from ganglion cells within each retina need to be synchronized, but must fire at separate times from the impulses generated by ganglion cells of the other eye (Stryker and Strickland, 1984, Invest. Ophthalmol. Vis. Sci. Suppl., abstract). Such activity patterns are thought to strengthen Hebbian synapses within the cortex, which can detect the correlations in firing among different inputs to the same cell (for reviews see Constantine-Paton et al., 1990; Shatz, 1990; Singer, 1990). We have recently provided evidence for correlated spontaneous firing in the isolated immature retina by monitoring the action potential activity of up to 100 neurons simultaneously with a microelectrode array (Meister et al., 1991). Cells in the developing ganglion cell layer spontaneously generate short periodic bursts of action potentials during the period when eye-specific layers are forming in the LGN. In addition, the firing of neighboring cells is highly synchronized, and during each burst of action potentials, the pattern of firing across the retina resembles a spatial wave that travels at several hundred micrometers per second.

The bursts of firing are very short with respect to the silent periods, which makes them well suited for instructing the process of eye-specific segregation during the development of retinogeniculate connections. In addition, local synchrony in the firing of neighboring retinal ganglion cells within the same eye could contribute to a refinement of topographic order within the retinogeniculate projection (Willshaw and von der Malsburg, 1976; for review see Shatz, 1990). However, for any retinal pattern of firing to be involved in these important processes, it must be present during the appropriate period of development. In the ferret, the eye-specific layers form during the first 3 postnatal weeks (Linden et al., 1981; Cucchiaro and Guillery, 1984). Here, we extend our multielectrode recording studies of the ferret retina to examine whether the spontaneous correlated bursting behavior is present during this critical 3 week period.

Even if the retina generates such patterned signals

*Present address: Vision, Touch and Hearing Research Center, University of Queensland, St. Lucia, Queensland 4072, Australia.
†Present address: Department of Cellular and Developmental Biology, Harvard University, Cambridge, Massachusetts 02138.
‡Present address: Division of Neurobiology, Department of Molecular and Cell Biology, Life Sciences Addition Room 221, University of California, Berkeley, Berkeley, California 94720.

at appropriate times, they can only be instructive in the ordering of projections to higher visual centers if they involve the ganglion cells, the only projecting neurons of the retina. In the cat and ferret retina, the ganglion cell layer contains not only ganglion cells, but a large population of interneurons, the displaced amacrine cells (Henderson et al., 1988; Wong and Hughes, 1987; Wässle et al., 1987), some of which fire action potentials (Freed et al., 1985; Bloomfield, 1992). Therefore, a second goal of our study was to establish the morphological identity of the bursting cells in the neonatal ferret retina. To do so, physiologically recorded cells were dye filled using intracellular electrodes. Taken together, our results suggest that the multielectrode recordings are indeed from ganglion cells whose pattern of firing is ideally suited to drive the activity-dependent process of segregation of their axonal terminals within the LGN.

Results

In the ferret dorsal LGN, the axon terminal arbors of ganglion cells projecting to the LGN from the two eyes overlap substantially prior to birth. At about postnatal day 4 (P4), the right and left eye arbors are first seen to occupy separate zones, signaling the onset of segregation. This eye-specific segregation continues throughout the first 3–4 postnatal weeks, and by P28, the distributions of left and right eye arbors become entirely restricted to their appropriate layers (Linden et al., 1981; Cucchiaro and Guillery, 1984). The retina itself is highly immature at birth: only a thin inner plexiform layer is present above a distinct ganglion cell layer. Few conventional synapses can be seen at P4, and ribbon synapses from bipolar cells do not appear until about P15. Membranous disks in the outer segments take shape between the second and third postnatal weeks, and the eyes are open at about P30 (Greiner and Weidman, 1981). Thus, the 4 weeks following birth in ferret constitute the period in which ganglion cell axons form eye-specific LGN layers and also mark the time of extensive functional maturation of retinal circuitry. We have recorded neural activity in the retinal ganglion cell layer from ferrets aged between birth and P30 and present the results in three parts. First, we examine age-related changes in the temporal and spatial patterns of firing of cells in the retinal ganglion cell layer of ferrets. Next, we demonstrate that many of the cells that fire action potentials are indeed ganglion cells. Finally, we consider more quantitatively the nature of the correlated firing of ganglion cells and age-related changes in these correlations.

Developmental Changes in the Spatial and Temporal Pattern of Activity

Cells in the ganglion cell layer of the ferret retina generated rhythmic bursts of action potentials as early as birth (P0), several days before eye-specific layers in the ferret LGN begin to appear. At this early stage, cells fired action potentials spontaneously in short bursts, 1–4 s long, as shown in Figure 1 (P0). These bursts were separated by long quiet periods; the average duration of these pauses was about 70 s, but occasionally bursts were separated by shorter intervals lasting 12–20 s. During a burst, cells fired at rates between 7 and 52 Hz. Such rhythmic bursting behavior persisted from birth to about the third postnatal week (Figure 1; Table 1). During this period, several aspects of the pattern of firing changed gradually. For example, as shown in Table 1, the maximal duration of individual bursts essentially doubled from 4 s at P0 to 7–9 s for some cells at P15–P21. At the same time, recordings at 35°C–36°C indicated that the average interburst interval declined significantly from 60–100 s at early ages to 28 s at P21. Table 1 also shows that the interburst interval decreased with increasing temperature at which the recordings were performed (compare interburst interval of P21a and P21b).

A dramatic change in the pattern of spontaneous activity was apparent by P30, about 3 days before eye opening in ferrets. At this age, the bursting activity of all cells was less rhythmic than in younger animals, and the short bursts were no longer consistently separated by long silent periods. Some cells even fired continuously, at a rate of 1–46 Hz, close to the firing rates we observed in adult animals (2–32 Hz).

During the first 3 postnatal weeks, these rhythmic bursts were highly synchronized among the majority of cells (Figure 1). Not all cells, however, participated each time activity was observed in the recorded population; sometimes, only a subset of cells (<50%) fired action potentials, forming "minor" bursts in the population (Figure 1, arrows). In a given experiment, these minor bursts could occur anywhere between 15% and 50% of the time, with no obvious variation with age. We also found no obvious subpopulations that consistently generated a partial burst. However, whenever 2 or more cells fired bursts of action potentials, they were always temporally well correlated with each other. By P30, in contrast, the more random firing of individual cells resulted in a loss of synchrony in the activity of the cells recorded on the array.

When the exact onset of firing was compared for different cells on the electrode array, we found that the bursts were not precisely synchronous (Meister et al., 1991); some cells started or ended their bursts before other cells, with time delays of up to 3 s. To determine whether this temporal sequence was related to the cells' spatial locations, we displayed the activity over the electrode array as a sequence of "movie frames," each frame representing a 0.5 s interval during a burst of action potentials.

Examples of such movies recorded from a P5 retina are shown in Figure 2. Inspection of any one frame demonstrates that nearby cells tended to fire synchronously, at times when distant cells were silent. Moreover, the activity in the population progressed across the retina in a spatially organized manner resembling an excitatory wave. In burst 3, for instance, cells began

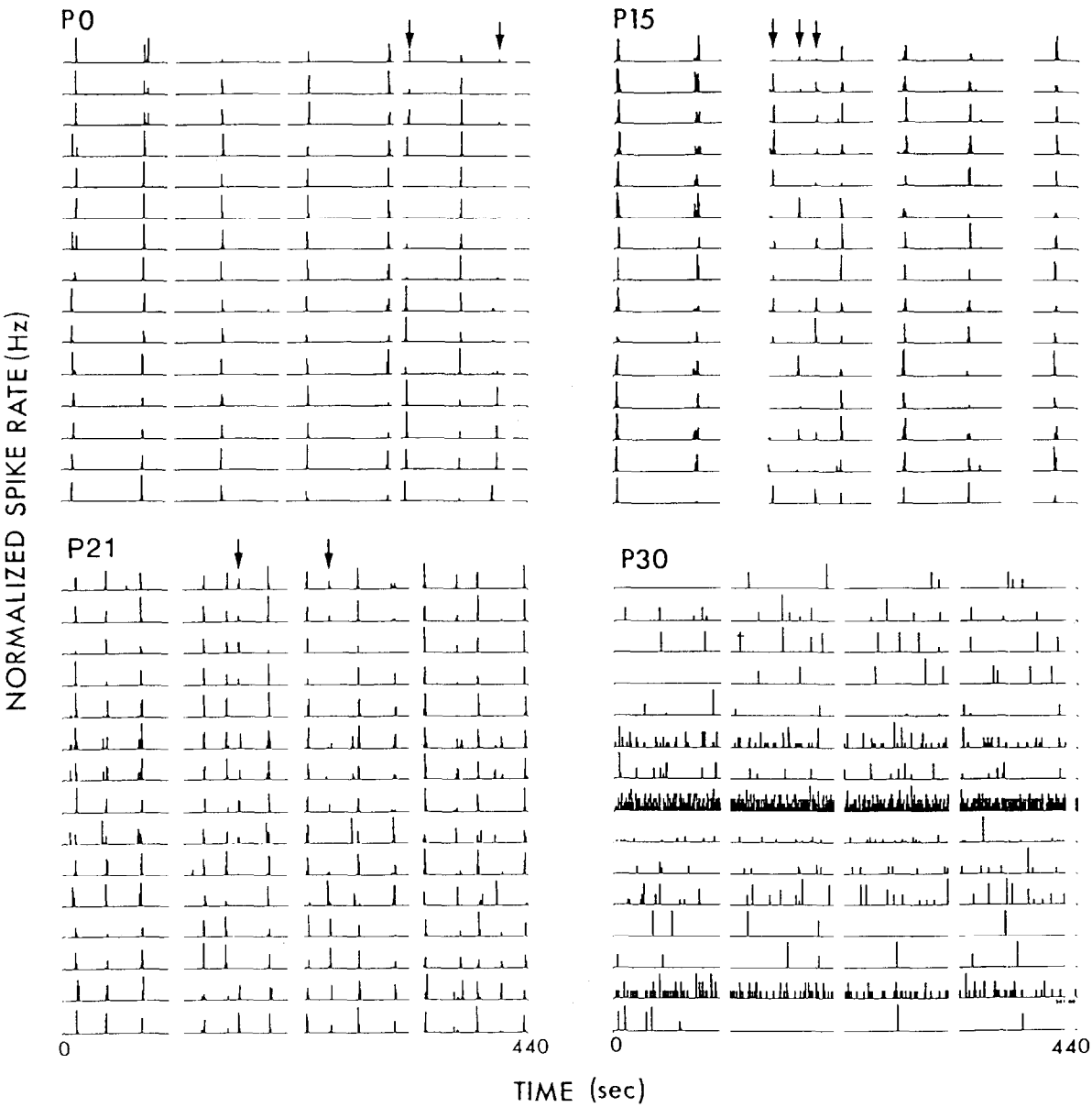

Figure 1. Firing Rate as a Function of Time for 15 Representative Neurons in the Retinal Ganglion Cell Layer of P0–P30 Ferrets

For each neuron, the spikes were binned at 1 s intervals, and the height of the resulting histogram was normalized to the maximum spike rate observed for that cell. Short breaks in the horizontal axes represent pauses in the recording process. Arrows indicate minor bursts in which only some cells participate.

firing at the left side of the array; subsequently, the activity swept across the array from lower left to upper right. Although the patterning of activity during a burst of firing was almost always wave-like, the direction of propagation of each wave varied as shown in the four examples of Figure 2. Not all cells recorded on the array participated in every wave. For instance, during burst 1, virtually no cells on the far left side of the array fired action potentials at any time, whereas many did so in burst 2. In bursts 3 and 4, all cells became active, but each wave propagated in a different direction. In addition, a wave involving only a subset of the recorded cells, such as the wave in burst 1 (Figure 2), tended to be followed by a wave that involved mainly the cells that were silent in the first burst (Figure 2, burst 2).

These waves of activity were a robust phenomenon and characteristic of at least 90% of all bursts recorded in each experiment. Most of the waves traveled straight across the region of the retina recorded by our electrode array, but on rare occasions, waves followed a circular trajectory. The speed of the wavefront could be estimated from the movie frames by measuring the time taken for the wave to travel from one corner of the array to the opposite corner, where it disappeared. For each burst of activity, we also ob-

Table 1. Multielectrode Recordings

Age	No. of Cells	Burst Duration (s)	Mean Interburst Interval (s)	Mean Firing Rate (Hz)	Range of Firing Rates (Hz)
P0	39	1–4	74 ± 6	29 ± 13	7–52
P1	44	1–4	70 ± 11	29 ± 14	9–54
P4	62	1–3	90 ± 16	14 ± 7	3–43
P5	65	2–4	101 ± 20	14 ± 7	3–36
P12a	45	2–7	71 ± 20	27 ± 14	9–65
P12b	59	2–6	77 ± 8	15 ± 9	4–39
P15a	49	2–6	71 ± 13	29 ± 18	6–92
P15b	73	2–7	60 ± 9	21 ± 11	2–53
P21a	50	2–9	28 ± 3	28 ± 20	6–86
P21b	75	2–10	48 ± 3[a]	15 ± 6	3–36
P30a	59	Some periodic bursts separated by 0.5–1 s intervals, or continuous firing		9 ± 4	1 –23
P30b	30	Some periodic bursts or continuous firing		11 ± 12	1–46
Adult	57	Some periodic bursts separated by 0.5–1 s intervals, or continuous firing		9 ± 7	2–36

A summary of the quantitative parameters describing the pattern of spontaneous activity in the retinal ganglion cell layer of postnatal and adult ferrets. Each row represents the results of recordings from a retinal piece taken from a separate animal.
[a] All retinas recorded at 35°C–36°C, except for P21b, which was recorded at 30°C. In one experiment, P21a, we varied the temperature between 26°C and 36°C and found a systematic variation in the average interburst interval as a function of temperature. The interval was 85 s at 26°C, 45 s at 30°C, and 28 at 36°C.

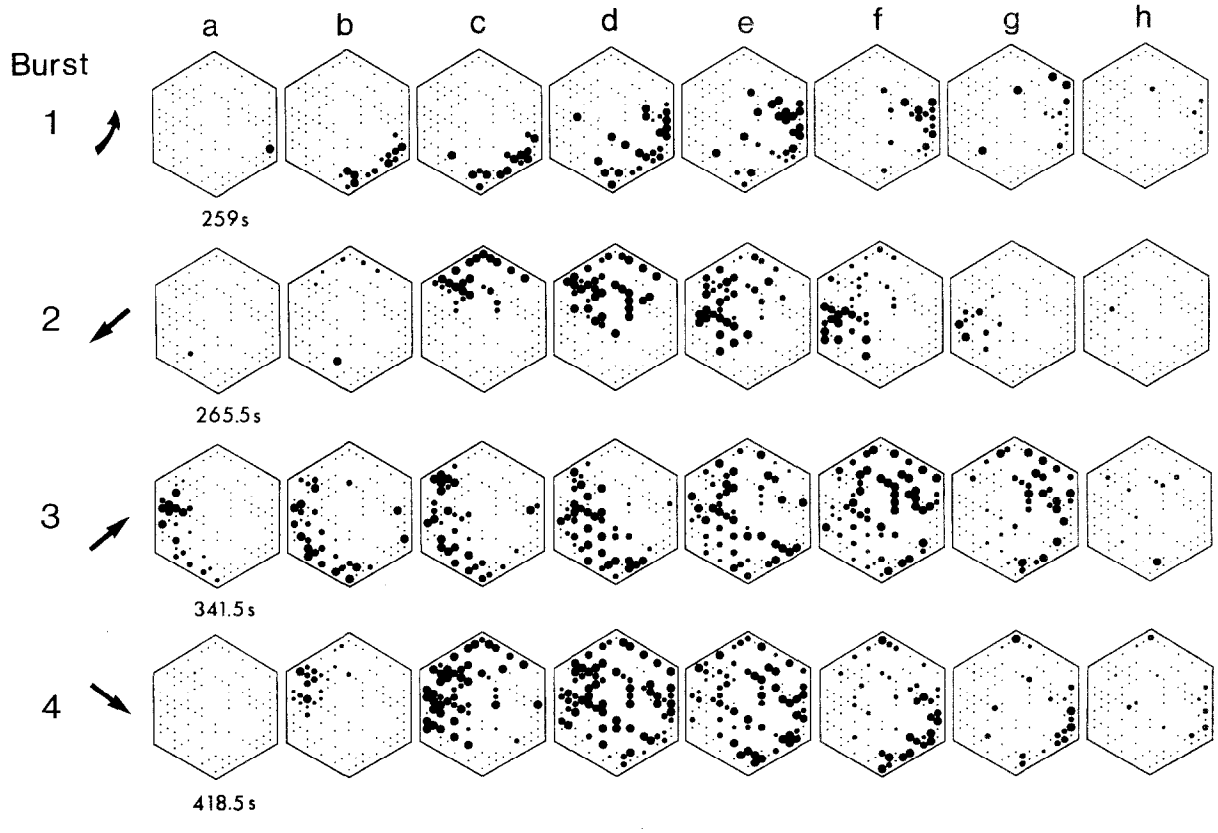

Figure 2. Spatial Progression of Spontaneous Activity during Four Consecutive Bursts from a P5 Retina

The boundary of the electrode array is depicted by a hexagon. Each recorded neuron is plotted by a dot at the estimated location of the cell body. The area of this dot varies in proportion to the firing rate of that neuron, normalized to the highest observed value. Frames (a)–(h) depict the mean firing rates in successive 0.5 s intervals. The time from the start of the experiment is given below the initial frame of each segment. Arrows indicate the estimated direction of propagation of the wave of activity.

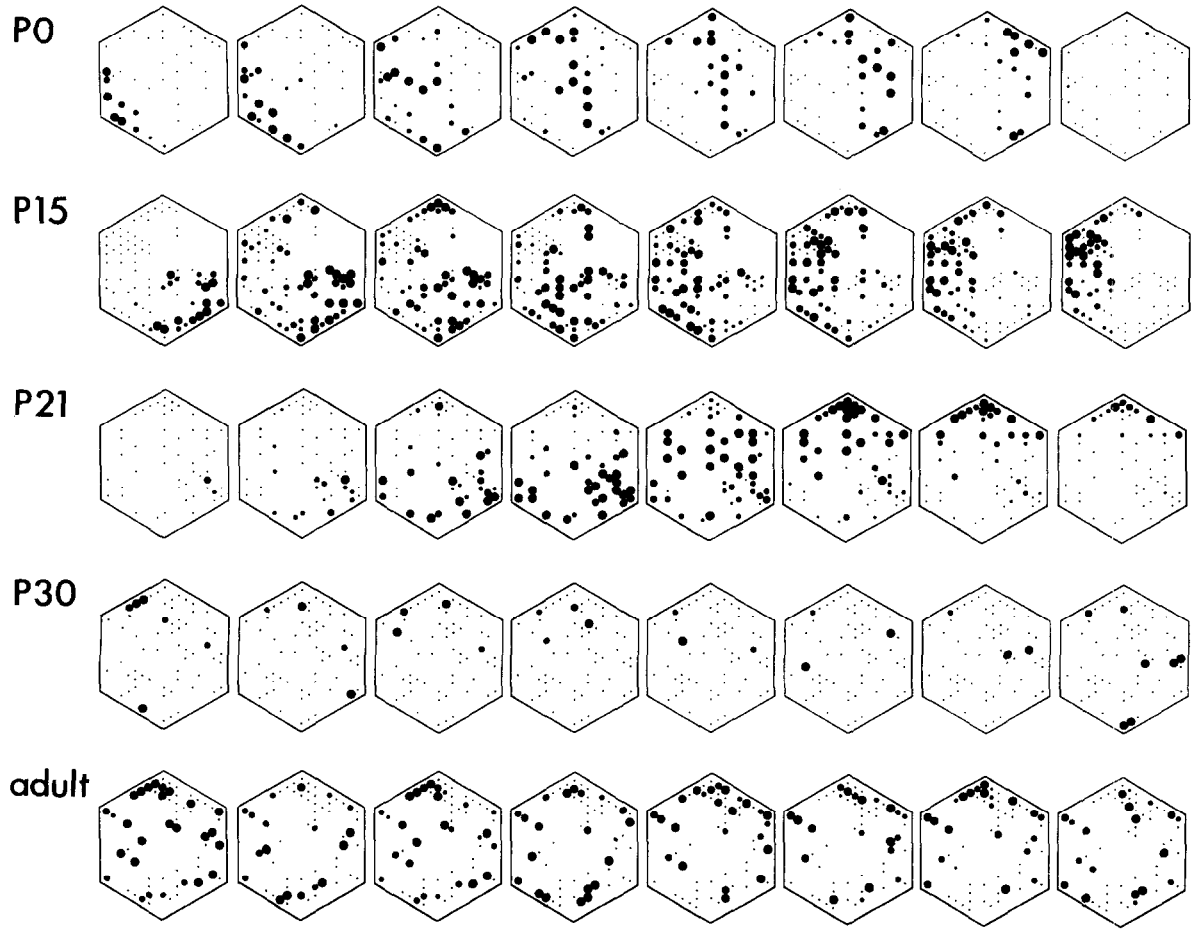

Figure 3. Representative Patterns of Activity in Retinas of Different Ages, Ranging from P0 to Adult

Sequences of firing activity in the ganglion cell layer were plotted as described for Figure 2. For ages P0, P15, and P21, we selected 4 s intervals that included a burst of activity. Since retinas at P30 and in adult animals no longer exhibited bursting activity, the corresponding 4 s periods were chosen at random. Recordings at P30 and for the adult were performed in the dark.

tained the wave speed by comparing the time delay in the peak firing of pairs of cells with the distance between the cells, measured in the direction of propagation of the wave. In general, the waves traveled at speeds between 150 and 300 μm/s and varied within this range from burst to burst in the same piece of tissue. However, this range of wave speeds did not vary with age.

The characteristics of the spatiotemporal patterning of retinal activity described above at P5 were common to all ages from birth (P0) to P21. As shown in the examples of Figure 3, waves of activity were present during this developmental period. Qualitative inspection of the waves suggests that the speed of the waves appeared essentially unchanged during the first 3 postnatal weeks, but the waves appeared to broaden between P0 and P5, consistent with the observation that the burst duration also increases during this time (Table 1; see also Figure 1). The waves also occurred more frequently with increasing age up to P21. However, by P30, waves could no longer be detected, nor were they present in the adult dark-adapted retina (Figure 3: P30, adult).

Identity of Bursting Neurons in the Ganglion Cell Layer

Action potentials were recorded with single microelectrodes from identified cells in the neonatal ferret retinal ganglion cell layer. Cells in this layer had resting membrane potentials between −55 and −45 mV. Subsequently, the soma and dendrites were dye filled to obtain the morphological identity (Figure 4; Figure 5; Figure 6). These recordings indicated that all major classes of ganglion cells exhibited rhythmic bursting behavior in the early neonates. The ganglion cells were identified based on similarities of dendritic morphology with adult ferret retina (Vitek et al., 1985; Wingate et al., 1992) and the presence of an axon in the optic fiber layer. An example of an intracellular recording from a β-like ganglion cell is shown in Figure 5. Over a period of 20 min, the bursts recorded from this cell varied between 2 and 5 s in duration, and the

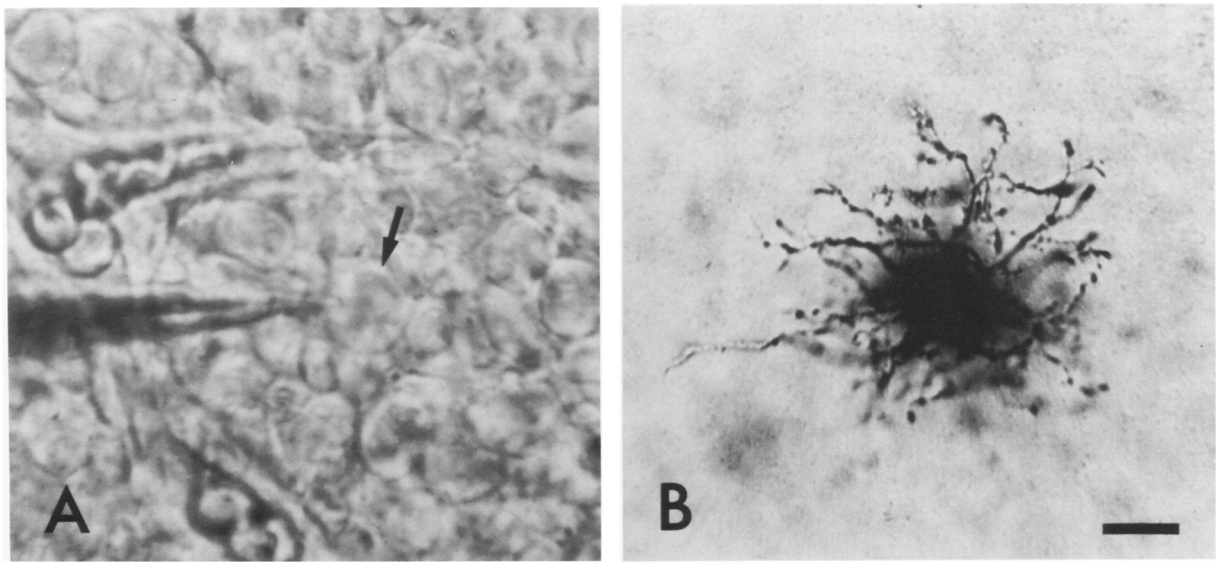

Figure 4. Recording and Dye Filling of Retinal Ganglion Cells

(A) Photomicrograph of the ganglion cell layer of a P11 ferret retina using Hoffman modulation contrast optics. An extracellular recording electrode is located adjacent to the soma of a cell (arrow), whose dendritic tree was subsequently stained by iontophoresis of Lucifer yellow using a second intracellular pipette. In some cases, cells were recorded intracellularly prior to dye filling. (B) The dendritic tree of the recorded cell in (A) revealed after photooxidation of the Lucifer yellow fill. This cell resembles a β ganglion cell in the adult ferret retina. By varying the focus, the axon could be traced into the optic fiber layer. Bar, 10 μm.

average interburst interval was about 50 s. All bursts of action potentials recorded from ganglion cells were associated with a large depolarization potential that lasted between 10 and 15 s (e.g., Figures 5C and 5D).

The durations of the bursts and interburst intervals from all cells studied in these single-cell recordings were similar to those observed at equivalent ages from the multielectrode recordings (compare Table 1 and Table 2). Occasionally, we recorded from cells with very small soma diameters of 5–8 μm that showed resting membrane potentials of about −50 mV, but no action potentials or rhythmic changes in membrane potential. When these cells were dye filled, their morphology and lack of an axon suggested that they were displaced amacrine cells. It is conceivable that impalement damaged the ability of these small cells to exhibit spontaneous changes in membrane potential, since many such cells died soon after impalement.

These recordings with single electrodes confirmed our earlier observation that the rhythmic bursting behavior of ganglion cells disappears between P28 and P30. At P28, some β ganglion cells still possessed clear

Table 2. Single Cell Recordings

Postnatal Week	No. of Cells	Range Burst Duration (s)	Mean Interburst Interval (s)
β ganglion cells			
2 (P7–P14)	i = 2	1–2	47.5 = 3.5
3 (P15–P20)	i = 5, e = 3	1–4	52.4 ± 13.2
4 (P23–P28)	i = 3, e = 2	1–4	29.6 = 7.3
≥5 (P29–P37)	i = 1, e = 2	Continuous firing at 1–3 Hz	
α ganglion cells			
2	0	–	–
3	i = 2	0.5–4	42.4 ± 7.4
4	i = 2	1.5–2	22.7 ± 1.7
≥5	i = 7, e = 1	Continuous firing at 1–8 Hz	
γ ganglion cells			
2	i = 1	2–5	40
3	i = 2	1–3	55.0 ± 21.2
4	i = 2, e = 1	1–4	36.7 ± 11.5
≥5	i = 1	Continuous firing at 2–4 Hz	

Patterns of spontaneous activity in the ganglion cell layer of postnatal ferrets, obtained from intracellular (i) and extracellular (e) recordings. All the cells listed here were demonstrated to possess an axon after dye injection, confirming that they were ganglion cells.

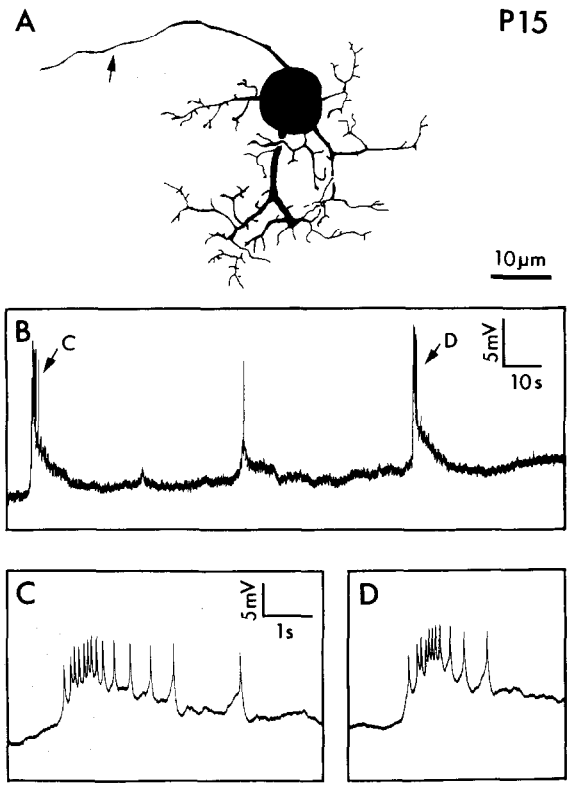

Figure 5. Intracellular Recording and Dye Filling of a β Ganglion Cell in a P15 Ferret Retina

(A) Camera lucida drawing of the cell filled with Lucifer yellow (arrow = axon).

(B) Intracellular recording from the cell body of this neuron.

(C and D) Portions of the record in (B), including bursts of action potentials, plotted on an expanded time base.

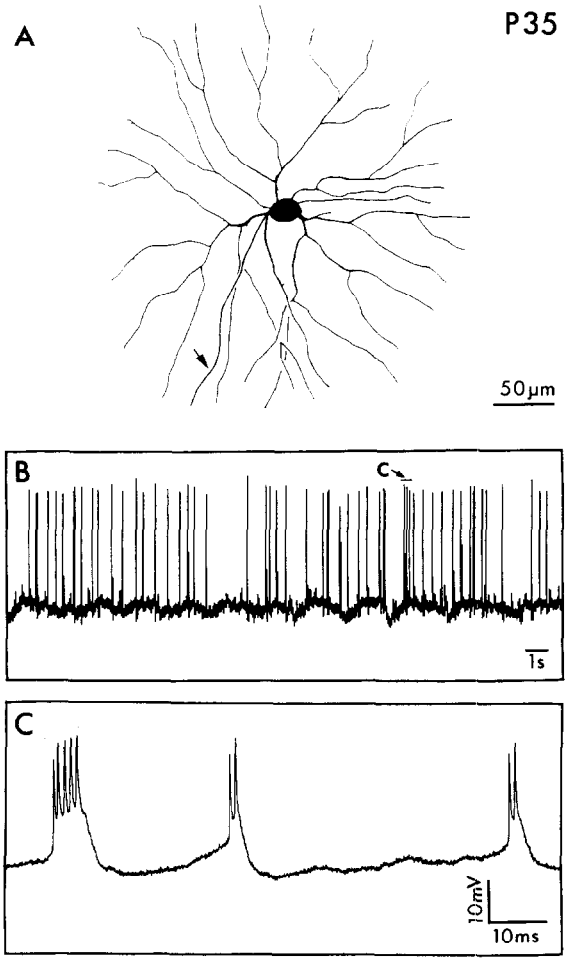

Figure 6. Intracellular Recording and Dye Filling of an α Ganglion Cell in a P35 Ferret Retina

(A) Camera lucida drawing of the cell filled with Lucifer yellow (arrow = axon).

(B) Intracellular recording from the cell body of this neuron.

(C) Portion of the record in (B), plotted on an expanded time base, showing doublets and multiplets of action potentials.

rhythmic bursting activity, whereas small γ ganglion cells and large α-like cells were much less rhythmic. By P30–P37, the majority of ganglion cells failed to burst rhythmically and, instead, had maintained firing rates of 1–10 Hz, comparable to those seen in the multielectrode records (see Figure 6B and Figure 1 at P30). At all ages, the ganglion cells identified morphologically as α ganglion cells fired doublets or multiplets of action potentials, 1–2.5 ms apart, each time the cell became depolarized (Figure 6C). Some γ ganglion cells also fired action potentials in doublets, but such a pattern of firing was never observed in β ganglion cells. Cells with this characteristic spiking pattern were sometimes observed in the multielectrode recordings as well. Thus, the single-cell recordings suggest that at least part of the rhythmic bursting activity detected by the multielectrode array derives from retinal ganglion cells. They also confirm that the rhythmic spiking behavior disappears from all cells by the fourth postnatal week.

Quantitative Measures of Correlation Strength

The basic assumption behind activity-dependent modification is that two synapses onto a common target cell can strengthen each other if their presynaptic inputs are simultaneously active (Constantine-Paton et al., 1990; Shatz, 1990; Brown et al., 1990). If the input fibers are of two distinct types, for example from the left and right eyes or from two distant regions within the same eye, and fibers of one type fire synchronously with each other but out of synchrony with the other type, then the fibers will gradually segregate from each other within their targets. As a result, each target cell ultimately receives inputs from only one fiber type (Miller et al., 1989). The precise timing rules by which two spiking inputs can reinforce each other are not known, but it is likely that their postsynaptic potentials must overlap in time. From studies of long-term potentiation (LTP) in the hippocampus, it appears that spikes from two fibers need to arrive within 0.05–0.10 s of each other to produce lasting enhancement (Gustafsson and Wigstrom, 1986; Madison et al., 1991).

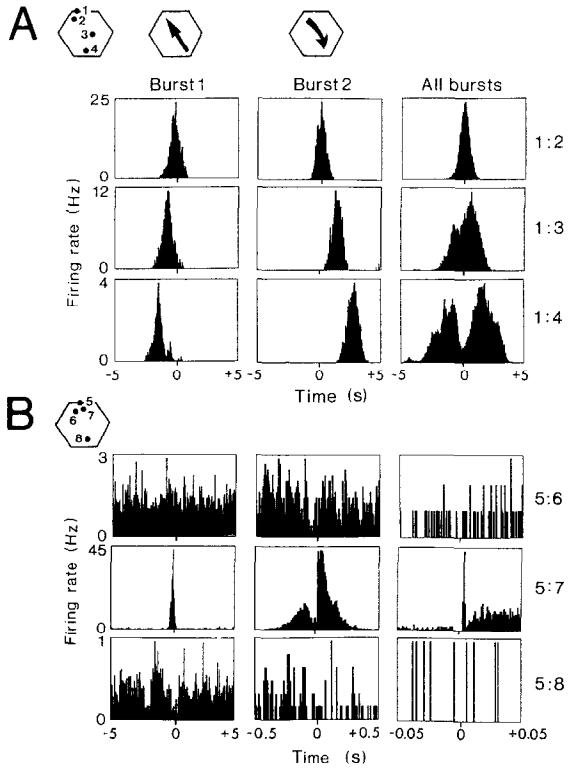

Figure 7. Cross-Correlation Functions between Pairs of Ganglion Cells Recorded on the Array at P0 or P30

(A) Pairwise cross-correlation functions between the spike trains of 4 cells in a P0 retina. The locations of the reference cell, labeled 1, and 3 other cells, labeled 2, 3, and 4, are indicated over an outline of the electrode array. Each plot represents the firing rate of cell 2, 3, or 4 as a function of time before or after an action potential from cell 1. The left and center columns of plots were computed for single bursts, during which the wave of activity traveled across the electrode array in the direction indicated at the top. Plots in the right column were computed over the entire 1055 s duration of this recording, including 19 different bursts.

(B) Pairwise cross-correlation functions between the spike trains of 4 cells in a P30 retina, defined as described in (A). All plots were computed over the entire 1090 s duration of this recording. The three columns show the same function on different time scales.

Such a mechanism can explain topographic map refinement or eye-specific segregation of retinal inputs to the LGN only if neighboring ganglion cells within the same retina frequently fire within 0.05–0.10 s of each other; and if ganglion cells from different retinas or at distant locations within the same retina are much less likely to fire within this correlation interval. To learn more about these quantitative aspects of retinal activity, we computed a cross-correlation function for every pair of spike trains recorded from the neurons on the electrode array. Such a correlogram represents the rate of firing of 1 cell as a function of time before and after an action potential from the other cell.

Figure 7A shows typical correlation functions among 4 cells recorded at P0: correlograms calculated during a single burst of action potentials showed a single peak. For a pair of neighboring cells (1:2), this peak was always centered near zero, indicating that the 2 neurons fired in near synchrony, regardless of the direction in which the wave of activity traveled. For a pair of distant cells (1:4), the correlation peak was most often displaced to earlier (burst 1) or later (burst 2) times. This delay corresponds to the time it took the wave of activity to propagate from 1 cell to the other. When the wave traveled in the opposite direction, the delay changed signs.

Between P0 and P21, the vast majority of pairwise correlation functions showed rather broad peaks with a full width at half maximum of 0.7–1 s. We found no sharp correlations on the millisecond scale, such as those observed between cells monosynaptically connected to each other (Mastronarde, 1983). The width of the correlograms did not appear to vary with intercellular distance.

To assess the correlation structure between spike trains over the longer time scales of synaptic refinement, we also computed correlograms averaged over many successive bursts (Figure 7A, all bursts). For pairs of nearby cells (1:2), the peak of their correlations remained near zero. By contrast, the correlograms for widely separated cells were broader and sometimes formed several peaks (1:3 and 1:4). This is because successive waves of activity propagated in different directions, resulting in varying time delays between the firing of 2 distant cells. On closer inspection, it was found that each of the 19 waves leading to Figure 7 took one of only six distinct trajectories. During this limited set of activity patterns, cell 1 was always activated either before or after cell 4, because none of the waves traveled in a direction perpendicular to their separation. This is reflected in the dip of the cross-correlogram near t = 0 in Figure 7A (all bursts). However, distant cell pairs from recordings in other retinas often showed cross-correlograms with more than two peaks and no dip at t = 0.

The disappearance of synchronous firing by the fourth postnatal week was confirmed by the cross-correlograms shown in Figure 7B. For a great majority of cell pairs, the time-averaged correlogram showed no peaks or other outstanding temporal structures on a scale of milliseconds to seconds for near neighbors (e.g., 5:6) and distant cell pairs (e.g., 5:8), suggesting that cells at P30 fire independently of each other. Similar flat cross-correlograms were observed in the adult retina (data not shown). However, in very few instances (<1% of all pairs), in P30 and adult retinas, the firing of 2 cells was highly correlated on the millisecond time scale. For example, the correlogram for cells 5 and 7 in Figure 7B shows that the firing rate of cell 7 increased significantly 5 ms after an action potential from cell 5. This resembles the correlations observed occasionally in the spontaneous firing of ganglion cells of the dark-adapted adult cat retina (Mastronarde, 1983) and may result from a direct synaptic interaction between the 2 ganglion cells. The above observations show that during the first 3 postnatal

weeks, nearby retinal ganglion cells are strongly correlated in their firing for interspike time delays between −0.5 and +0.5 s. This range certainly includes the ±0.05 s time interval expected to be relevant for long-term synaptic enhancement.

Figure 7 also demonstrates that distant pairs of cells are less correlated in their firing than are neighbors. To examine this relationship quantitatively, we measured the effective correlation for each pair by means of the following procedure. For each pair of recorded cells, we computed a ratio of correlation by counting the number of times a spike from 1 cell occurred within ± 0.05 s of a spike from the other cell on the assumption that only such spike pairs will be effective in enhancing a common synaptic connection. This number was then divided by the number of such qualifying spike pairs that would be obtained if these 2 cells were firing at the same average rates but without any temporal correlation. The ratio of these two numbers yields a correlation index that measures how strongly the 2 neurons are correlated compared with the equivalent 2 neurons if they were firing randomly with respect to each other. A correlation index of 1 indicates that the 2 cells are firing independently, such as the pairs of cells 5:6 and 5:8 shown at P30 in Figure 7B. An index greater than 1 implies that cells are more likely to fire within ±0.05 s than expected by chance, such as the cell pair (1:2) at P0 in Figure 7A. An index less than 1 would imply that the 2 cells tend not to fire together.

Figure 8 shows the result of such calculations for recordings from a P0 retina and is based on an analysis of 778 cell pairs. For every pair of recorded neurons, we computed the correlation index as described above (see also Experimental Procedures) and plotted the resulting value as a function of the retinal distance between the 2 cell bodies. This scatter plot shows that the largest values of the correlation index are found for pairs of near neighboring cells, which are up to 100 times more correlated by this measure than expected by chance. The degree of correlation generally declines with increasing intercellular distance. At distances beyond 500 μm, many neurons are essentially uncorrelated on the critical time scale of ±0.05 s. Though the correlation tends to decrease with distance, this relationship clearly is not perfect, and at any given distance, the correlation index can vary considerably for different cell pairs.

The spatial dependence of the correlation strength was found to change considerably throughout development, as illustrated in Figure 9. The correlation index is plotted as a function of intercellular distance for retinas of four different ages: P0, P15, P30, and adult. Each curve was derived from a computation similar to that illustrated in Figure 8, but the data points were pooled into bins of 20 μm along the distance axis. Each plot reveals that the spatial dependence of the correlation index is well approximated by an exponential decline. The y-intercept of these exponential fits, which is the correlation index expected for nearest neighboring ganglion cells, decreases systematically with age. The slope of the fit also varies with age. We shall define the correlation distance as the distance over which the correlation index falls by 1/e, which is inversely proportional to the slope of the regression line. Figure 9 suggests that this correlation distance increases systematically with age.

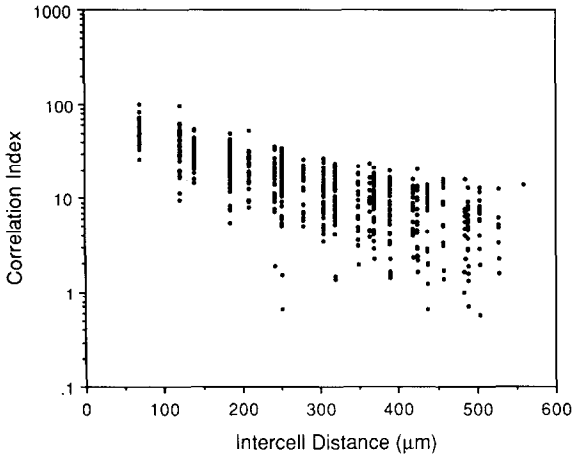

Figure 8. Correlation Index as a Function of Distance in a P0 Ferret Retina

For each pair among 39 recorded spike trains, the correlation index i_{AB} was computed as described in Experimental Procedures and plotted logarithmically against the retinal distance between the 2 cell bodies. A total of 778 cell pairs were analyzed.

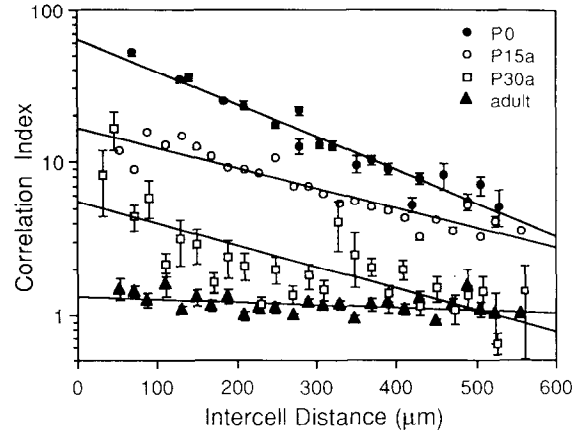

Figure 9. Correlation Index as a Function of Distance in Ferret Retinas at Four Different Ages

For each pair of recorded spike trains, the correlation index i_{AB} was computed as described in Experimental Procedures and plotted logarithmically against the retinal distance between the 2 cell bodies. For a compact representation, the values for individual cell pairs were averaged over bins of 20 μm width along the distance scale. The error bars show the standard deviation of the correlation index values in each bin. Also shown are exponential fits to the data. The total numbers of cell pairs analyzed for the curves were 778 (P0), 1703 (P15a), 992 (P30a), and 1395 (adult).

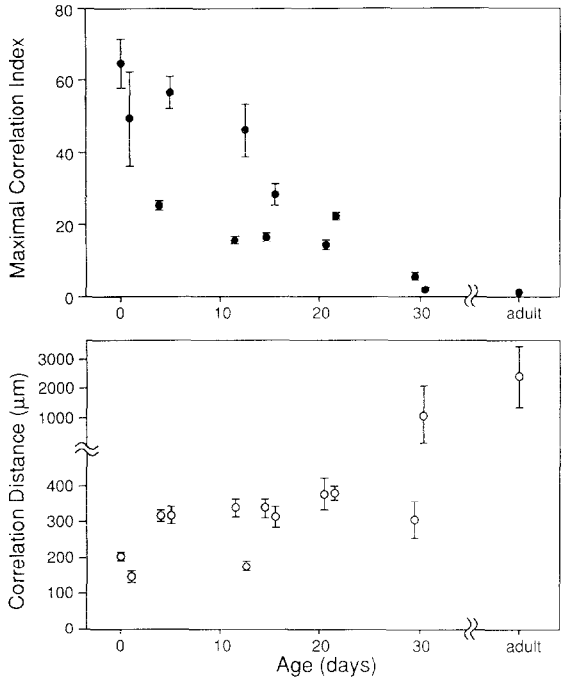

Figure 10. Dependence of the Correlation Index and Correlation Distance on Age

For each retina, the dependence of the correlation index on intercellular distance was fitted exponentially as illustrated in Figure 9. The maximal correlation index is defined as the y-intercept of that regression line. The correlation distance is defined as the distance over which the exponential fit decreases by a factor of e and is thus inversely proportional to the slope of the regression line. Error bars correspond to the uncertainty in these fitting parameters. A total of 22,845 cell pairs were analyzed from retinas of 13 animals.

These relationships are revealed more clearly in Figure 10, which summarizes our analysis of 22,845 cell pairs from 13 retinas. For each retina, the maximal correlation index and the correlation distance were derived from exponential fits as in Figure 9. These two parameters are plotted against the age of the experimental animal. Apparently, the strength of the correlations is highest in the youngest retinas. Between P0 and P21, the period when waves are present, the maximal correlation index gradually declines by about a factor of 3, although at P21 nearby cells are still 20 times more likely to fire together than expected by chance. During this time, the spatial extent of the correlations doubles after the first postnatal week, and then remains essentially unchanged. At P30, the correlation index is even less dependent on intercellular distances; however, cells closest to each other still have a 4–6 times greater chance of firing within ± 0.05 s of each other than if they fired independently (see also Figure 9). By adulthood, the correlation index at all distances varies between 1 and 2, indicating that at this age cells are firing essentially independently of each other. Although there is a clear systematic dependence of these parameters on age, there is also some variability among experimental animals with the same or very similar age. This variability appears to be more pronounced for the strength of the correlation than for its spatial decay distance.

Discussion

A major goal of this study was to examine the time course of development of correlated bursting activity of cells in the ganglion cell layer of the retina during the period in which ganglion cell axons are known to segregate according to eye preference within the LGN. Many separate lines of experiments have suggested that precise spatial and temporal patterning of action potentials arising from the retinal ganglion cells is required for the terminals of ganglion cell axons to segregate into layers and to form a highly ordered topographic map (for reviews see Constantine-Paton et al., 1990; Shatz, 1990). Using a multielectrode recording technique that permits us to examine the firing of many cells simultaneously, we previously demonstrated that appropriate patterns of activity are indeed present in the developing ferret retina (Meister et al., 1991): neighboring cells in the retinal ganglion cell layer generate bursts of action potentials that are highly correlated with one another, even before visual stimulation is possible. In addition, the spatial patterning of activity is in the form of an excitatory wave that propagates across the retina in various directions from burst to burst. Here, we have extended these observations first by demonstrating that many, if not all, of the cells recorded on the multielectrode array are indeed retinal ganglion cells rather than retinal interneurons, such as amacrine cells. Moreover, we have shown that the rhythmic bursting activity and waves are present throughout the period in which only ganglion cell axons are known to refine their connections within the LGN, from the day of birth to at least P21. But the waves disappear by P30, just a few days before eye opening. Finally, a quantitative analysis of the spatiotemporal pattern of firing indicates that there is a steady decline in the strength of correlations between neighboring cells until adult levels are reached at the end of the period of axonal refinement.

Reports from other authors suggest that the patterns of activity recorded in our experiments are not merely the result of damage to the retina in the course of the isolation procedure. Recordings from the retinas of fetal rats showed that ganglion cells in vivo fire in rhythmic bursts, similar to those seen here on the multielectrode array, and that neighboring cells are broadly correlated in their firing (Galli and Maffei, 1988; Maffei and Galli-Resta, 1990). Periodic bursting activity can also be recorded in vivo from target neurons in the neonatal rabbit superior colliculus (Spear et al., 1972) and LGN (Rapisardi et al., 1975), and it appears to originate from retinal ganglion cells because blockade of impulses from the eye prevents the rhythmic firing of the target neurons. Although these observations argue strongly that the rhythmic burst-

ing behavior of ganglion cells seen on the array is physiologically normal, they cannot address directly the issue of whether such bursts entail a wave-like progression of neural activity in vivo. However, we can conclude from the presence of waves in our recordings that the retina contains the physiological and anatomical substrates to generate such distinct spatial patterns of correlated activity. The specific wave-like nature of retinal activity patterns could be tested directly by in vivo recordings with two electrodes. Comparing the activity from sites at various retinal distances should produce the characteristic correlograms pictured in Figure 7. So far, our attempts at such measurements have failed for lack of a suitable anesthetic. In particular, halothane and ketamine were found to depress significantly the activity in retinas from neonatal ferrets, both in vivo and in vitro.

Identity of Cells Recorded by the Electrode Array

Our recordings and dye filling using single microelectrodes show that ganglion cells belonging to the major morphological classes can generate the rhythmic bursting pattern of firing. Although we never found displaced amacrines to spike, it is still possible that these cells also contribute to the spikes recorded on the array. Some amacrine cells are known to spike in the adult rabbit retina (Bloomfield, 1992), but we rarely obtained stable recordings from the displaced amacrine cells over sufficiently long periods of time to determine whether they showed periodic slow membrane depolarizations with or without action potentials. Even if other cell types should participate in the waves of activity, the fact that at least some ganglion cells are involved implies that these correlated signals are transferred to the LGN. Since patterned spontaneous activity also occurs in retinal ganglion cells of the rat (Galli and Maffei, 1988; Maffei and Galli-Resta, 1990) and cat (R. O. L. Wong, M. Meister, and C. J. Shatz, unpublished data), it is likely that this activity has a common role in the development of retinogeniculate projections across species and is not unique to the ferret.

The Development of Spontaneous Retinal Activity Patterns

The patterns of firing of retinal ganglion cells change in several ways during the period between birth and P30. The waves of excitation traveling across the retina become progressively broader in older animals, resulting in longer bursts of action potentials produced by individual cells. Furthermore, the waves occur more and more frequently as the retina matures, resulting in shorter quiet intervals between the bursts generated by individual neurons. The adult retina no longer exhibits burst-like modes of activity: it appears that the waves have broadened and become more frequent to the point of merging into a continuous maintained level of activity without spatial or temporal structure. One parameter remained constant throughout development: the propagation velocity of the wave of excitation, which ranged from 150 to 300 μm/s in any given preparation without dependence on the animal's age.

Of particular interest for the development of the retinogeniculate projection are the temporal correlations between the spike trains of different retinal ganglion cells. Several aspects of these correlation functions can be derived at least qualitatively from the above description of the wave patterns. For instance, the cross-correlograms indicate that nearby ganglion cells are strongly correlated in their firing over time intervals of the order of the burst duration (Figure 7A; Table 1). For each burst, as the separation between the 2 cells increases, the peak of the correlogram shifts away from $t = 0$. This displacement of the correlogram peak is comparable to the time taken by a wave to cross the distance between the 2 cells.

We also calculated a correlation index that measures how much more 2 cells are correlated over the critical time interval of ± 0.05 s than expected for 2 similar cells firing independently of each other. Because the observed bursts tend to be significantly longer than this 0.1 s time interval, one can easily estimate the correlation index from the wave properties. For a pair of nearby bursting neurons, the index is simply the inverse of the cells' duty cycle, which is the fraction of time the cells are active. This expectation is confirmed by a comparison of Table 1 and Table 2. The correlation index decreases as the separation between the 2 cells increases, because the wave takes a finite time to travel across this distance. Once the cells are separated by about one wave width, the number of spike pairs arriving within the critical ± 0.05 s of each other is significantly reduced. In fact, our measured values of the decay distance for the correlation index correspond to approximately the width of a wave and show the same increasing trend with age (see Table 1 and Table 2). Finally, with increasing age, the waves become broader and more frequent. This change in the firing pattern increases the probability for chance coincidences between spikes from 2 uncorrelated cells and thus progressively reduces the correlation index.

How Are the Waves of Excitation Generated and Controlled?

The results reported here can only indirectly address the question of how the waves are generated, but our observations place certain constraints on any hypothesis. The fact that the waves move very slowly across the retina (about 150–300 μm/s) implies that excitation is not propagated by fast chemical synapses or conventional high conductance electrical gap junctions. This suggestion is supported by the broadness of the cross-correlograms, which are typically ± 0.5 s in width, far broader than expected if cells were only synaptically driven or coupled electrically via high conductance gap junctions (Mastronarde, 1983; Ts'o et al., 1986). The waves may result from the slow extracellular diffusion of an excitatory substance such as

K^+ or a neurotransmitter. Since the Müller glial cells, which in the adult control K^+ and neurotransmitter homeostasis in the extracellular space, are likely to be immature in the young neonates (Redburn et al., 1992), neurotransmitters or K^+ released during an action potential may remain in the extracellular space for a sufficiently long period of time to excite neighboring cells, causing further release of transmitters or K^+. Alternatively, the waves may spread from cell to cell by diffusion of messenger molecules through intercellular junctions as seen in networks of astrocytes (Cornell-Bell et al., 1990; Finkbeiner, 1992). Intracellular junctions are also found among neurons in the adult rabbit and cat retina (Vaney, 1991). Preliminary studies show that the small molecule neurobiotin can also pass across junctions between ganglion cells and other ganglion cells and amacrine cells in the developing ferret retina (Penn et al., 1992, Soc. Neurosci., abstract).

The observed development of neural activity patterns throughout the first few weeks of life may result from changes in the membrane properties of single neurons, or from changes in the structure of their interconnections. For example, under the above hypothesis of regenerative diffusion, maturation of the glial cells throughout this period may gradually alter the volume and concentrations in the extracellular space, thus changing both the excitability of ganglion cells and the conditions for diffusion of excitatory substances. If, on the other hand, the waves of excitation are sustained by a more specific network of connections, our observations would suggest that this network undergoes significant changes between birth and P30. In fact, there is anatomical evidence for the progressive development of synaptic circuitry of retinal ganglion cells during this period. At P0, there are very few synapses of any kind within the inner plexiform layer of the retina, whereas by P30, just before eye opening, a significant number of ribbon synapses thought to be from bipolar cell terminals are present (Greiner and Weidman, 1981). These findings, taken in conjunction with our own observations here, suggest that perhaps an early horizontal network responsible for correlating the activity of retinal ganglion cells is not dismantled but, rather, is overridden by a maturing vertical circuit from photoreceptors through bipolars to ganglion cells. Since the photoreceptors release transmitter in the dark, this vertical circuit is spontaneously active and would be expected to interfere with the correlations mediated by horizontal connections in the ganglion cell layer.

Implications for the Refinement of Retinogeniculate Projections

A major finding of this study is that the waves of activity are present throughout the period during which the ganglion cell axon terminals are refined both according to eye preference and topographic position within their target structures (Sretavan and Shatz, 1986, 1987; Cucchiaro and Guillery, 1984; Jeffery, 1985). These synaptic rearrangements in the LGN are known to depend on electrical activity in the optic nerve. It has been suggested that the process is driven by a Hebbian mechanism of synaptic enhancement, in which two fibers connecting onto the same target neuron can reinforce each other's synapses if they carry correlated electrical signals (Willshaw and von der Malsburg, 1976; Miller et al., 1989). The patterns of neural activity reported here have the qualitative properties to drive such a correlation-based mechanism, because 2 ganglion cells within the same retina are more strongly correlated in their firing than 2 cells from opposite eyes; and nearby ganglion cells are more strongly correlated than widely separated cells. The remainder of this section will examine these statements quantitatively.

In developing a quantitative measure of correlation, we assumed that the mechanism of activity-dependent refinement in the LGN resembles other known instances of LTP. From studies of LTP in the hippocampus, it appears that two terminals can interact to strengthen their synapses if they are active within 0.05–0.1 s of each other (Gustafsson and Wigstrom, 1986). Thus, we took the essential correlation event to be a pair of spikes from 2 cells occurring within a time interval of less than 0.05 s. For any given pair of cells, the correlation index, i_{AB}, indicates how often such an event occurs, compared with how often it would occur for similar cells firing randomly with respect to each other. Thus, we expect the correlation index for a pair of cells located in opposite eyes to be 1.0, on the assumption that the two eyes support similar patterns of activity but are not temporally synchronized. This seems a reasonable assumption for several reasons. First, there are no known connections between mammalian ganglion cells in the two eyes either during development or in the adult. Nor is there a known efferent projection common to both retinas. Finally, the patterns of firing within each retina are highly variable in their timing and direction of propagation, such that even spurious correlations between the two eyes are unlikely to persist for a significant period.

These considerations suggest that ganglion cells at birth are up to 65 times more correlated in their firing than similar cells taken from opposite eyes. This results primarily from the fact that the synchronous bursts of action potentials are about 65 times shorter than the quiet intervals that separate them. This should provide a very strong bias in any Hebbian mechanism to favor multiple connections from the same eye to a given target neuron. The correlation index decreases gradually with age, but remains above 10 throughout the critical first 3 weeks of life. After P30, this correlation measure approaches 1, indicating an absence of eye-specific correlations on the ± 0.05 s time scale. By this time, the retinogeniculate projection has stabilized, eye-specific correlation signals are no longer required, and the retina matures to its primary function: to transmit visual images.

At every age except in adult animals, we find that the correlation index decreases significantly with intercellular distance. This is due to the finite propagation velocity of the waves of activity. Nevertheless, even cell pairs separated by 500 μm show a correlation index above 5 from P0 to P21. Because of the limited extent of our electrode array, we did not assess correlations at larger retinal distances, but it seems plausible that the index drops to unity beyond about 1 mm. Thus, two fibers from ganglion cells 1 mm apart would enjoy no advantage in competing for LGN neurons over two fibers deriving from opposite eyes. However, since the earliest retinogeniculate projection is probably already organized according to a coarse topographic map, by analogy with studies in lower vertebrates (for reviews see Constantine-Paton et al., 1990; Udin and Fawcett, 1990), such competition between widely separated neurons is unlikely to occur in practice.

This discussion illustrates that the patterns of bursting activity may also act to reinforce the topographic accuracy of the retinogeniculate projection. For example, at P0, 2 ganglion cells separated by 200 μm are less than half as strongly correlated as near neighboring ganglion cells. Thus, a correlation-based mechanism of synaptic enhancement would favor nearby ganglion cells connecting to the same area in the LGN. As a result, the initially rough topographic projection might become gradually more refined. There is a limit to this improvement, set by the distance dependence of the correlation index: We would expect that this type of mechanism cannot produce a retinal resolution much finer than the decay length of the correlation index. This quantity increases from about 175 to 300 μm between P0 and P5, thereafter it changes little up until P30. However, the retina grows during this time, increasing the spacing between neighboring ganglion cells, with a 2-fold decrease in cell density in midperipheral retina (P5 and P21; Henderson et al., 1988). Thus, a circle with a radius of 1 decay length contains only half as many ganglion cells at P21 as at P5. As a result, LGN neurons may receive inputs from a progressively more restricted population of retinal ganglion cells, thereby sharpening the retinotopic map.

More detailed speculations for the development of the retinogeniculate projection will require a better understanding of the synaptic mechanisms in these structures. For example, our correlation index merely computes the relative factor by which 2 cells are more correlated than the equivalent 2 cells from opposite eyes, but takes no note of the absolute firing rates. In our experiments, the absolute firing rate often varied by a factor of 10 over the recorded population of neurons. Since we do not know how the firing rate of the presynaptic terminals affects the correlation-based enhancement, it is difficult to proceed to more quantitative predictions, such as the degree of eye-specific segregation that can be supported by these firing patterns.

Similarly, we do not know what the requirement for temporal coincidence might be at these immature synapses. Clearly, the observed patterns of activity are not precisely tuned to the 0.05–0.1 s integration times reported in studies of hippocampal LTP: the bursts of action potentials typically last from 1 to 5 s. As a result, one computes about the same values for the correlation index assuming a coincidence interval of ±0.5 s, as for the interval used here (±0.05 s). Thus, these patterns of activity could support equally well a correlation-based mechanism with a synaptic integration time of 0.5 s, but would be less efficient for much larger correlation windows. A recent study of NMDA receptor–mediated currents at the synapse between developing rodent retinal ganglion cells and neurons of the superior colliculus indicates that elementary postsynaptic currents last significantly longer than in the adult (Hestrin, 1992). In addition, early retinogeniculate synapses are ultrastructurally immature and contain very few synaptic vesicles (Campbell and Shatz, 1992). Thus, it is possible that the entire process of synaptic transmission and hence synaptic strengthening is slower during development, resulting in a longer integration time than for hippocampal LTP. In a preliminary study of retinogeniculate synapses in slices of neonatal ferret LGN, we have recently obtained evidence for a long lasting increase in synaptic transmission following stimulation of the optic tract, similar to that generated by the retinal ganglion cells (Mooney et al., 1993). We hope that this preparation will shed more light on the integrative properties of these synapses.

The waves of activity seem ideally suited to drive the refinement of the topographic map and the eye-specific segregation of ganglion cell axons in the LGN. However, other aspects of retinogeniculate development, also thought to depend on the spontaneous firing of ganglion cells prior to eye opening, are not as easy to understand. In particular, each LGN neuron tends to receive inputs from ganglion cells of only one type, e.g., on-center or off-center, α or β cells; blocking activity in neonatal cats or ferrets prevents this further refinement in ganglion cell connectivity (Dubin et al., 1986; Hahm et al., 1991). If these subtypes also segregated by a correlation-based mechanism, we would have expected the ganglion cell population to split into two or more subgroups, with strong correlations in firing between cells of the same subgroup, but not across subgroups. We found no evidence for such effects. It is possible that these final refinements in the precision of the retinogeniculate projection require the very robust correlations that are generated only at the onset of vision. This would be consistent with the observation that cat ganglion cell axons continue to undergo a progressive restriction of their terminal arbors within the LGN up to 3 months postnatally (Sur et al., 1984), well after eye opening at about P10. Further experiments are needed to resolve the extent to which spontaneously generated versus visually driven activity contributes to the final patterning

of retinogeniculate connections. Nevertheless, the present observations underscore that the spontaneous waves of activity are a powerful source of correlations suitable for activity-dependent synaptic modification prior to vision.

Experimental Procedures

Multielectrode Recordings

Adult ferrets and neonates aged between P0 and P30 were anesthetized with Nembutal (20 mg/kg) prior to removal of the eyes (the number of retinas used at each age is summarized in Table 1; the results from each animal are tabulated separately). In each experiment, the retina was dissected from the eyecup in oxygenated Ames medium (+20 mM HEPES; Sigma, H-3375; Ames and Nesbett, 1981). This culture medium most closely resembles the fluid in which the rabbit retina is bathed in vivo; it contains the usual inorganic salt components (120 mM NaCl; 3.1 mM KCl; 0.5 mM KPO_4, 1.2 mM $MgSO_4$, 1.2 mM $CaCl_2 \cdot 2H_20$) together with amino acids and vitamin supplements, as well as 6 mM glucose, and is used routinely in electrophysiological recording studies of the adult retina (Yang and Masland, 1992). We find essentially no differences in spike patterns for retinas recorded in Ames medium compared with physiological Ringer's solution, but the retinas remained healthy in Ames medium for much longer periods of time. In adult ferrets, the dissection was done under infrared optics after the animals were dark adapted for 30 min–2 hr.

A square piece of retina, 3–4 mm in width, was cut from a region midway between the nerve head and the peripheral margin of the retina and placed ganglion cell side down onto a cover glass containing a flat array of 61 extracellular electrodes spaced 70 μm apart from each other and arranged in a hexagonal pattern, with a total diameter of about 0.5 mm (Meister et al., 1991; see also Regehr et al., 1989). During each recording session, we often recorded from more than one quadrant of the same retina (always in midperipheral retina). Because we found no obvious differences in the pattern of activity between different quadrants of the same retina, we did not make any attempt to record consistently from one particular quadrant. The array of electrodes was enclosed by a small well in which the retina could be perfused with oxygenated Ames medium. The piece of retina was held down either with a fine nylon mesh or a dialysis membrane. The temperature of the perfusate was kept at 35°C–37°C by heating the inlet perfusion pipe with a heating coil and the base of the chamber with a flow of heated air that was regulated using a temperature controller (Omega, CN 9122). Recordings of the adult retinas were performed in the dark, and those of neonatal retinas were carried out in a dimly lit room.

Under these conditions, the retina remained physiologically stable for up to at least 10 hr. During this time, the 61 electrodes registered action potentials simultaneously from between 50 and 100 neurons, each electrode recording from up to 3 different cells. The spikes were recorded, sorted, and analyzed as described by Meister et al. (1991, 1993). For each identified neuron, these procedures provided a continuous spike train throughout the recording period, as well as an estimate of the location of the cell body over the electrode array.

Single-Cell Recordings

To identify cells that fired spontaneous action potentials, retinas from ferrets (P10–P37) were isolated and placed ganglion cell side up in a perfusion chamber mounted on the stage of an upright fluorescence microscope (Zeiss). The retinas were kept flat by adhering onto a piece of black filter paper (Millipore, HABP 045) that was secured into the chamber by two side clamps. Small 1 mm^2 holes in the filter paper allowed examination of the retina with transilluminated light, and the ganglion cell layer was clearly visualized using Hoffman Modulation Contrast Optics. The tissues were kept alive by superfusing with oxygenated Ames medium (Sigma) warmed to 32°C–35°C by two Peltier devices that provided heating to the microscope stage and chamber.

Intracellular electrodes with a final resistance of 100–150 MΩ were filled with 2.5% carboxyfluorescein (Kodak, #9953) or sulforhodamine (Molecular Probes, Catalog #S-359) in 0.1 M potassium acetate and were positioned next to a cell in the ganglion cell layer using a 40× water immersion objective (Zeiss), corrected for Hoffman Optics. A stepper motor (Newport) enabled fine placement of the electrode adjacent to a chosen cell that was then impaled following capacitive ringing. After recording several cycles of action potential bursts (10–30 min), the cells were iontophoretically filled with dye (+1–2 nA, continuous) and photographed immediately. In some cases, the fluorescent staining was later converted to a permanent 3,3' diaminobenzidine tetrahydrochloride reaction product, visible in the light microscope, by photooxidation (Maranto, 1982).

It was often difficult to obtain stable intracellular recordings from the neonatal cells because of their small size and also because the dense extracellular matrix of internal limiting membrane prevented easy access to the underlying ganglion cells. Thus, extracellular recordings were also performed, using glass micropipettes (2–5 MΩ) containing Ames medium or 3% NaCl. Clear imaging of cells using Hoffman Optics allowed us to center the recorded cell in the middle of the cross-hair of a graticule in the eyepiece, which subsequently enabled the recorded cells to be impaled with a second intracellular pipette containing 5% Lucifer yellow in 0.1 M LiCl (−1 nA, continuous). Voltage signals from the electrodes were amplified by a Getting Amplifier, sampled by a Neurocorder (Neurodata DR-484), recorded by a videocassette recorder, and monitored by an oscilloscope. The recorded action potentials were then digitized and plotted.

Analysis of Neural Spike Trains

To estimate the firing rate of a neuron recorded with the electrode array, we counted the action potentials in successive time bins and divided these counts by the bin width. The resulting estimate of firing rate as a function of time, $r_A(t)$, was displayed either in the traditional histogram form (Figure 1) or by the size of a dot in the spatial display of activity (Figure 2; Figure 3). To give an indication of the relative variations in firing, each cell's firing rate was normalized to its maximal value.

The cross-correlation function between the spike trains of 2 neurons A and B, $c_{AB}(t)$, was estimated by computing all time intervals between a spike from A and a spike from B, binning these into successive time bins and dividing the result by the total number of spikes from A and the bin width. This yields an estimate of the firing rate of cell B as a function of time since an action potential from cell A.

The correlation index between cell A and cell B, i_{AB}, measures the factor by which the firing rate of cell B increases over its mean value within ±0.05 s of a spike from cell A. We first determined the average firing rate of B within the interval of ±0.05 s around a spike from A, by counting the number of times a spike from B occurred within ±0.05 s of a spike from A and dividing the result by the total number of spikes from A and the width of the correlation interval, 0.1 s. This value was then divided by the overall mean firing rate of cell B, computed as the total number of spikes from B divided by the duration of the recording.

Formally, if

T = duration of the recording;

Δt = bin width;

$N_{A(t_1,t_2)}$ = number of spikes from cell A between times t_1 and t_2;

$N_{A(0,T)}$ = total number of spikes from cell A during the recording;

$N_{B(0,T)}$ = total number of spikes from cell B during the recording;

$N_{AB(t_1,t_2)}$ = number of spike pairs from cells A and B for which cell B fires within t_1 and t_2 of cell A,

then

$r_A(t)$ = firing rate of cell A at time t

$$= \frac{N_{A(t,t+\Delta t)}}{\Delta t}$$

$c_{AB}(t)$ = firing rate of cell B at time t after a spike from cell A

$$= \frac{N_{AB(t,t+\Delta t)}}{N_{A(0,T)} \cdot \Delta t}$$

i_{AB} = correlation index between cells A and B

$$= \frac{N_{AB(-0.05s,+0.05s)} \cdot T}{N_{A(0,T)} \cdot N_{B(0,T)} \cdot (0.1\ \mathrm{s})}.$$

Acknowledgments

We wish to thank Dr. Denis Baylor for providing us with guidance and encouragement and R. Schneeveis for technical support. This work was supported by NSF Grant IBN-9212640 and a grant from the March of Dimes to C. J. S., a C. J. Martin NHMRC Fellowship to R. O. L. W., and a Scholar Grant from the Lucille P. Markey Charitable Trust to M. M.

The costs of publication of this article were defrayed in part by the payment of page charges. This article must therefore be hereby marked "*advertisement*" in accordance with 18 USC Section 1734 solely to indicate this fact.

Received April 23, 1993; revised August 9, 1993.

References

Ames, A., and Nesbett, F. B. (1981). In vitro retina as an experimental model of the central nervous system. J. Neurochem. *37*, 867–877.

Bloomfield, S. A. (1992). Relationship between receptive and dendritic field size of amacrine cells in the rabbit retina. J. Neurophysiol. *68*, 711–725.

Brown, T. H., Kairiss, E. W., and Keenan, C. L. (1990). Hebbian synapses: biophysical mechanisms and algorithms. Annu. Rev. Neurosci. *13*, 475–511.

Campbell, G., and Shatz, C. J. (1992). Transient synapses formed by individual retinogeniculate axons during segregation of eye input in the cat. J. Neurosci. *12*, 1847–1858.

Cline, H. T. (1991). Activity-dependent plasticity in the visual systems of frogs and fish. Trends Neurosci. *14*, 104–111.

Constantine-Paton, M., Cline, H. T., and Debski, E. (1990). Patterned activity, synaptic convergence, and the NMDA receptor in developing visual pathways. Annu. Rev. Neurosci. *13*, 129–154.

Cornell-Bell, A. H., Finkbeiner, S. M., Cooper, M. S., and Smith, S. J. (1990). Glutamate induces calcium waves in cultured astrocytes: long range glial signaling. Science *247*, 470–473.

Cucchiaro, J., and Guillery, R. W. (1984). The development of the retinogeniculate pathways in normal and albino ferrets. Proc. R. Soc. Lond. (B) *223*, 141–164.

Dubin, M. W., Stark, L. A., and Archer, S. M. (1986). A role for action-potential activity in the development of neuronal connections in the kitten retinogeniculate pathway. J. Neurosci. *6*, 1021–1036.

Finkbeiner, S. (1992). Calcium waves in astrocytes—filling in the gaps. Neuron *8*, 1101–1108.

Galli, L., and Maffei, L. (1988). Spontaneous impulse activity of rat retinal ganglion cells in prenatal life. Science *242*, 90–91.

Greiner, J. V., and Weidman, T. A. (1980). Histogenesis of the cat retina. Exp. Eye Res. *30*, 439–453.

Greiner, J. V., and Weidman, T. A. (1981). Histogenesis of the ferret retina. Exp. Eye Res. *33*, 315–332.

Gustafsson, B., and Wigstrom, H. (1986). Hippocampal long-lasting potentiation produced by pairing single volleys and brief conditioning tetani evoked in separate afferents. J. Neurosci. *6*, 1575–1582.

Madison, D. V., Malenka, R. C., and Nicoll, R. A. (1991). Mechanisms underlying long-term potentiation of synaptic transmission. Annu. Rev. Neurosci. *14*, 379–397.

Maffei, L., and Galli-Resta, L. (1990). Correlation in the discharges of neighboring rat retinal ganglion cells during prenatal life. Proc. Natl. Acad. Sci. USA *87*, 2861–2864.

Maranto, A. R. (1982). Neuronal mapping: a photooxidation reaction makes Lucifer yellow useful for electron microscopy. Science *217*, 953–955.

Mastronarde, D. N. (1983). Correlated firing of cat retinal ganglion cells. I. Spontaneously active inputs to X- and Y-cells. J. Neurophysiol. *49*, 303–324.

Meister, M., Wong, R. O. L., Baylor, D. A., and Shatz, C. J. (1991). Synchronous bursts of action potentials in ganglion cells of the developing mammalian retina. Science *252*, 939–943.

Meister, M., Pine, J., and Baylor, D. A. (1993). Multi-neuronal signals from the retina: acquisition and analysis. J. Neurosci. Meth., in press.

Miller, K. D., Keller, J. B., and Stryker, M. P. (1989). Ocular dominance column development: analysis and simulation. Science *245*, 605–615.

Mooney, R., Madison, D. V., and Shatz, C. J. (1993). Enhancement of transmission at the developing retinogeniculate synapse. Neuron *10*, 815–825.

Rapisardi, S. C., Chow, K. L., and Mathers, L. H. (1975). Ontogenesis of receptive field characteristics in the dorsal lateral geniculate nucleus of the rabbit. Exp. Brain Res. *22*, 295–305.

Redburn, D. A., Agarwal, S. H., Messersmith, E. K., and Mitchell, C. K. (1992). Development of the glutamate system in rabbit retina. Neurochem. Res. *17*, 61–66.

Regehr, W. G., Pine, J., Cohan, C. S., Mischke, M. D., and Tank, D.W. (1989). Sealing cultured invertebrate neurons to embedded dish electrodes facilitates long-term stimulation and recording. J. Neurosci. Meth. *30*, 91–106.

Shatz, C. J. (1990). Impulse activity and the patterning of connections during CNS development. Neuron *5*, 745–756.

Shatz, C. J., and Stryker, M. P. (1988). Prenatal tetrodotoxin infusion blocks segregation of retinogeniculate afferents. Science *242*, 87–89.

Singer, W. (1990). The formation of cooperative cell assemblies in the visual cortex. J. Exp. Biol. *153*, 177–197.

Spear, P. D., Chow, K. L., Masland, R. H., and Murphy, E. H. (1972). Ontogenesis of receptive field characteristics of superior colliculus neurons in the rabbit. Brain Res. *45*, 67–86.

Sretavan, D. W., and Shatz, C. J. (1986). Prenatal development of retinal ganglion cell axons: segregation into eye-specific layers within the cat's lateral geniculate nucleus. J. Neurosci. *6*, 234–251.

Sretavan, D. W., and Shatz, C. J. (1987). Axon trajectories and pattern of terminal arborization during the prenatal development of the cat's retinogeniculate pathway. J. Comp. Neurol. *255*, 386–400.

Sretavan, D. W., Shatz, C. J., and Stryker, M. P. (1988). Modification of retinal ganglion cell axon morphology by prenatal infusion of tetrodotoxin. Nature *336*, 468–471.

Sur, M., Weller, R. E., and Sherman, S. M. (1984). Development of X- and Y-cell retinogeniculate terminations in kittens. Nature *310*, 246–249.

Ts'o, D., Gilbert, C. D., and Wiesel, T. N. (1986). Relationships between horizontal interactions and functional architecture in cat striate cortex as revealed by cross-correlation analysis. J. Neurosci. *6*, 1160–1170.

Udin, S. B., and Fawcett, J. W. (1988). Formation of topographic maps. Annu. Rev. Neurosci. *11*, 289–327.

Vaney, D. I. (1991). Many diverse types of retinal neurons show tracer coupling when injected with biocytin or neurobiotin. Neurosci. Lett. *125*, 187–190.

Vitek, D. J., Schall, J. D., and Leventhal, A. G. (1985). Morphology, central projections and dendritic field orientation of retinal ganglion cells in the ferret. J. Comp. Neurol. *241*, 1–11.

Wässle, H., Chun, M. H., and Müller, F. (1987). Amacrine cells in the ganglion cell layer of the cat retina. J. Comp. Neurol. *265*, 391–408.

Willshaw, D. J., and von der Malsburg, C. (1976). How patterned neural connections can be set up by self-organization. Proc. R. Soc. Lond. (B) *194*, 431–445.

Wingate, R. J. T., Fitzgibbon, T., and Thompson, I. D. (1992). Lucifer yellow, retrograde tracers, and fractal analysis characterise adult ferret retinal ganglion cells. J. Comp. Neurol. *323*, 449–474.

Wong, R. O. L., and Hughes, A. (1987). The morphology, number, and distribution of a large population of confirmed displaced amacrine cells in the adult cat retina. J. Comp. Neurol. *255*, 159–177.

Yang, G., and Masland, R. H. (1992). Direct visualization of the dendritic and receptive fields of directionally selective retinal ganglion cells. Science *268*, 1949–1952.